Z. Phys. B – Condensed Matter 75, 187–195 (1989)

Condensed Matter
Zeitschrift für Physik B

The influence of oxygen vacancies on the chemical bonding in titanium oxide*

F. Schlapansky, P. Herzig, R. Eibler, G. Hobiger, and A. Neckel
Institut für Physikalische Chemie, Universität Wien, Vienna, Austria

Received September 28, 1988; revised version November 28, 1988

A self-consistent LAPW band structure calculation for $TiO_{0.75}$ has been performed, assuming long-range order of vacancies on the oxygen sublattice. The calculation is based on a hypothetical model structure which can be described as $Ti_3^{[4]}Ti^{[6]}O_3\square_O$, where $\square_O$ denotes an oxygen vacancy. In the model structure two types of titanium atoms occur: $Ti^{[4]}$ atoms which have two vacancies as neighbours and are quadratically surrounded by four oxygen atoms, and $Ti^{[6]}$ atoms which are octahedrally surrounded by six oxygen atoms. The calculated density of states (DOS) and the local partial densities of states are compared with the respective values for stoichiometric TiO containing no vacancies. A characteristic difference is the appearance of two sharp peaks in the DOS curve below the Fermi energy which are caused by the vacancies. These "vacancy states" exhibit a considerable amount of charge in the vacancy muffin-tin sphere and are found to be derived from Ti 3*d* states extending into the vacancy sphere. The introduction of vacancies also leads to a lowering of the Fermi energy indicating a stabilizing effect. The bonding situation in $TiO_{0.75}$ as compared to TiO as well as the changes in chemical bonding in the series $TiC_{0.75}-TiN_{0.75}-TiO_{0.75}$ are discussed on the basis of electron density plots. The loss of $Ti^{[4]}-O$ bonds (as compared to TiO) is compensated by the formation of $Ti^{[4]}-\square_O-Ti^{[4]}$ bonds across the vacancy and by an increase of the bond strength of the $Ti^{[4]}-O$ bonds. On the other hand, the $Ti^{[4]}-Ti^{[4]}$ and particularly the $Ti^{[4]}-Ti^{[6]}$ bonds are weakened by the introduction of vacancies.

1. Introduction

Three phases are known for titanium oxide that contain the stoichiometric composition TiO [1]. Their structures are all closely related to the sodium chloride structure [2]. At temperatures below 940 °C, a completely ordered monoclinic modification is obtained [1, 3] having 16.7% vacancies on both sublattices (α-TiO). Between 940 °C and ca. 1250 °C the cubic β-TiO phase is stable [2] within a maximum range of ca. 47–55 at. % oxygen. Also this phase contains vacancies on both sublattices. However, the vacancies are not randomly distributed over all lattice sites, but only occur on particular sites which are statistically occupied. A cubic high temperature phase TiO_x is formed above about 1250 °C [1, 4] with a homogeneity range of $0.75 \leqq x \leqq 1.3$. In this phase (γ-TiO) the vacancies are randomly distributed. Roughly 15% vacancies on both sublattices are present for the stoichiometric composition, whereas at a composition of $x=0.75$ only about 5% vacancies at the metal sublattice are observed [4].

Several calculations of the electronic structure of TiO are available in the literature, some of them based on the LCAO method [5–7] and others on the APW method [8–10]. In all those calculations a sodium chloride structure without vacancies was assumed. A step towards more realistic structures was made by Schoen and Denker [11] who applied the "Virtual Crystal Approximation" (VCA) in connection with the APW method in order to calculate the band struc-

* Dedicated to Professor F. Kohler on the occasion of his 65th birthday

tures for a series of compositions, keeping the oxygen-titanium ratio constant at unity and varying the vacancy concentration, as well as keeping the vacancy concentration at approx. 15% and varying the oxygen-titanium ratio from 0.8 to 1.22. This method, however, can only give limited insight into the electronic structure of solids containing vacancies, since vacancy states, which are of crucial importance for the understanding of such compounds, are not obtained from such a treatment.

An Extended Hückel investigation of NbO and of α-TiO has been performed by Burdett and Hughbanks [12]. The authors have shown that the experimentally observed structures for both compounds cannot be understood from electrostatic considerations but are a consequence of their electronic structures.

Schwarz [13] recently published an ASW calculation for an ordered defect structure of TiO. In his paper, he compares the densities of states (DOS) for a series of oxides (MgO, Cu_2O, TiO, NbO, TiO_2 and RuO_2) without presenting a more detailed analysis of the bonding situation.

A very recent KKR-CPA calculation for TiO containing 15% vacancies randomly distributed over both sublattices has been performed by Hörmandinger et al. [14]. This paper gives the DOS together with the calculated X-ray emission spectra, the Auger spectra and the X-ray photoelectron spectra.

As a first step in a systematic investigation of the chemical bonding in titanium oxide, band structure calculations for an ordered model structure of $TiO_{0.75}$ are described in the present paper. Similar calculations have already been performed for $TiC_{0.75}$ [15, 16] and $TiN_{0.75}$ [17]. Together with the results of those calculations, the changing bonding properties going from the carbide to the oxide shall be discussed, whereby one has to keep in mind that in the carbide and in the nitride vacancies only occur on the nonmetal lattice, whereas for TiO vacancies on both the titanium and the oxygen lattices are observed. However, for the model structure used in the present paper, only vacancies on the oxygen sublattice are considered.

A theoretical investigation of the bonding situation in TiO, assuming an NbO structure with 25% ordered vacancies on both sublattices, will be given in a forthcoming paper [18].

2. Computational aspects

The present work is based on two calculations: One for the (hypothetical) ordered model structure $TiO_{0.75}$ ($Ti_3^{[4]}Ti^{[6]}O_3\square_O$) which is displayed in Fig. 1. In this

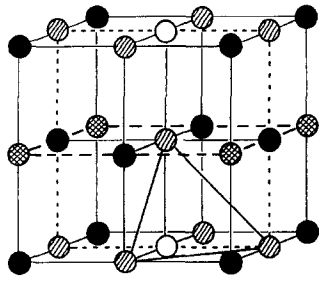

Fig. 1. Cubic unit cell for the model structure of $TiO_{0.75}$. ●: O atoms; ○: vacancies; : $Ti^{[4]}$ atoms; : $Ti^{[6]}$ atoms. — — —: (100) plane, cut 1; ...: (100) plane, cut 2; ——: (111) plane

Table 1. Input parameters for the LAPW band structure calculation of ordered $TiO_{0.75}$ and TiO (in a.u.)

Quantity	Region	$TiO_{0.75}$	TiO
Lattice parameters		7.9274	7.8927
Atomic sphere radii	$Ti^{[4]}$, $Ti^{[6]}$	2.1512	2.1418
	O, $\square_O$	1.8125	1.8046

structure the $Ti^{[4]}$ atoms are surrounded by four oxygen atoms and two oxygen vacancies $\square_O$, whereas the $Ti^{[6]}$ atoms have six nearest oxygen neighbours. The other calculation is for the sodium chloride structure of stoichiometric titanium oxide (in the following denoted as TiO). The band structure calculations have been performed using the self-consistent LAPW method [19, 20]. The muffin-tin approximation was used for the potential, whereas a general charge density in form of a Fourier expansion was used between the atomic spheres during the self-consistency procedure. The exchange-correlation potential was calculated according to Hedin and Lundqvist [21].

The lattice parameter of TiO_x decreases with increasing oxygen contents x. For TiO, the same lattice parameter as in [10] was used, whereas for $TiO_{0.75}$ the lattice parameter was taken from Banus et al. [4]. Table 1 shows the lattice parameters and the atomic sphere radii used in the present calculation. For $TiO_{0.75}$ energies and wave functions were calculated for 10 **k** points in the irreducible part of the Brillouin zone. One iteration with 165 **k** points was performed after having reached self-consistency in order to calculate the DOS. For TiO 29 **k** points were used throughout.

The **k** expansion was extended over 350 **k** vectors for $TiO_{0.75}$ and to a maximum of 40 for TiO. The l-expansion inside the muffin-tin spheres was taken up to $l=12$ for both calculations. In order to calculate the DOS and the l-like partial DOS the tetrahedron

method [22] was employed. The computation of the electron densities follows closely the formalism given in [16] except that unsymmetrized basis functions were used.

3. Results

a) Band structures and DOS

Figure 2 shows the band structures for TiO and for ordered $TiO_{0.75}$. A direct comparison is facilitated by folding back the face-centered cubic Brillouin zone for TiO into the simple cubic one. The band structure of TiO is in agreement with a previous calculation [10] which was performed using the APW method. In $TiO_{0.75}$ there are states with a relatively high amount of charge in the vacancy sphere ("vacancy states"). These states with *s* character in the vacancy sphere are encircled in Fig. 2b, and a charge analysis for 13 highly symmetric vacancy states is given in Table 2. As in the case of $TiN_{0.75}$, and as opposed to the corresponding carbide, all those states lie below the Fermi energy. Comparing the charges for the vacancy states of the substoichiometric carbide, the nitride and the oxide, a continuous increase of the vacancy charge can be observed, which is more pronounced between the carbide and the nitride. The comparison, however, has to be performed in such a way that the different volumes of the vacancy spheres are taken into account, particularly when going from the nitride to the oxide whereby the vacancy sphere volume decreases by about 20%. The increasing electronic charge in the vacancy sphere will later be interpreted as a strengthening of the $Ti^{[4]}-\square_O-Ti^{[4]}$ bonds.

The DOS curves for TiO and for ordered $TiO_{0.75}$ are given in Fig. 3. The first peak at low energy is predominantly formed by oxygen 2*s* states ("*s* band"), the second peak has mainly oxygen 2*p* character ("*p* band"). The DOS above the energy gap is chiefly caused by Ti 3*d* states ("*d* band") and its peak structure is characteristically changed by the introduction of vacancies. For $TiO_{0.75}$ the occurrence of additional peaks below the Fermi level ("vacancy peaks") is caused by the introduction of oxygen vacancies and can be understood in connection with the above-mentioned vacancy states and with the $Ti^{[4]}-Ti^{[4]}$ bonds across the vacancy sphere. As for titanium carbide

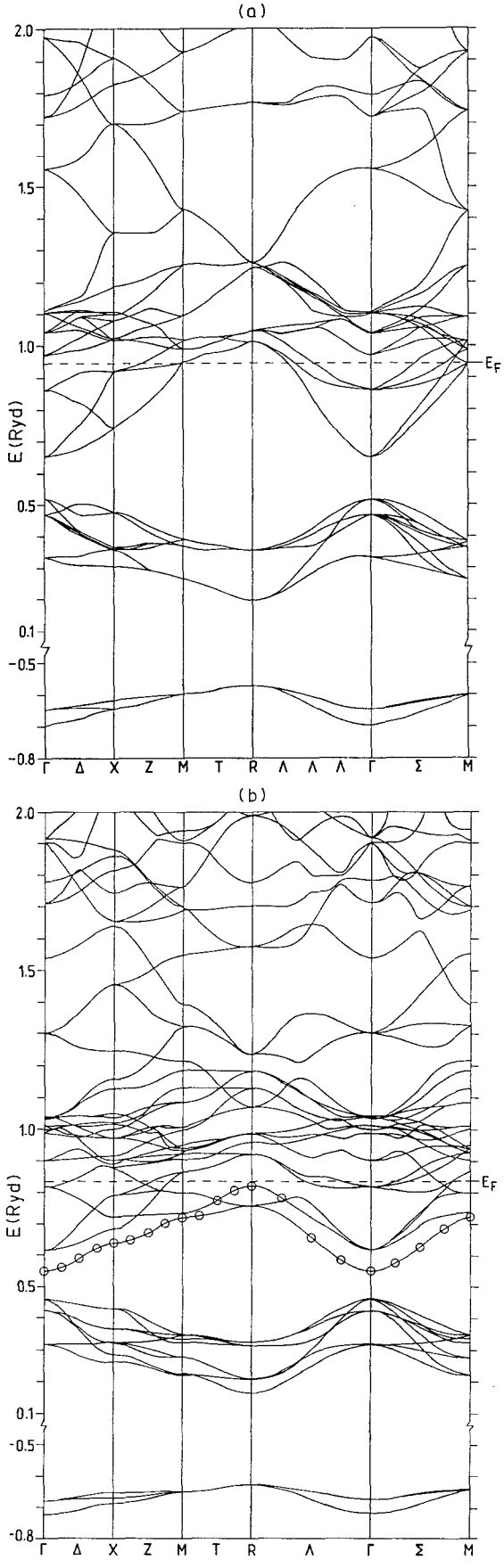

Fig. 2a and b. Band structure of TiO (**a**) and ordered $TiO_{0.75}$ (**b**). The band structure of TiO has been backfolded into the smaller Brillouin zone of the simple cubic lattice. So-called vacancy states are encircled in **b**. Energies with respect to the constant muffin-tin potential between the spheres

Table 2. Charge analysis for some vacancy states of ordered $TiO_{0.75}$. Upper part: bonding states; lower part: antibonding states

Irr. rep.	E (Ryd.)	O sphere total	$Ti^{[4]}$ sphere								$\square_O$ sphere			$Ti^{[6]}$ sphere total	q_{out}
			s	p	d	d_{z^2}	$d_{x^2-y^2}$	d_{xy}	(d_{xz}, d_{yz})	total	s	p	total		
Γ_1	0.5460	1.80	10.02	–	27.28	27.28	–	–	–	37.33	22.05	–	22.06	0.13	38.68
Δ_1	0.5900	4.64	7.46	0.96	30.67	30.08	0.59	–	–	39.15	20.94	0.28	21.27	0.20	34.74
X_1	0.6369	3.98	5.24	2.47	34.45	32.93	1.52	–	–	42.25	21.32	–	21.53	0.01	32.23
Z_1	0.6698	3.71	4.35	3.66	34.82	33.60	0.82	–	0.40	42.93	20.43	0.50	21.11	0.04	32.21
M_1	0.7197	3.69	2.41	6.71	32.29	32.29	–	–	–	41.51	21.30	–	21.61	0.25	32.94
T_1	0.7718	1.39	0.41	11.25	28.30	3.10	–	–	25.20	39.98	14.22	0.61	14.93	0.58	43.12
R_1	0.8201	1.43	–	19.62	–	–	–	–	–	19.63	25.28	–	25.30	0.18	53.45
Δ_1	0.6549	4.14	4.99	2.38	35.71	33.09	–	0.33	2.29	43.19	17.94	1.42	19.40	0.76	32.51
Σ_1	0.6245	4.58	6.05	1.92	32.99	32.17	0.44	0.11	0.27	41.05	20.10	0.68	20.84	0.26	33.27
S_1	0.6979	4.10	3.46	3.43	39.47	33.83	0.32	–	5.32	46.47	16.47	1.72	18.31	0.13	30.99
$M_{5'}$	0.7970	4.59	2.19	0.75	59.93	29.13	1.04	–	29.76	63.14	–	5.24	5.29	0.13	26.85
$X_{4'}$	0.8871	1.40	3.61	1.56	59.67	59.67	–	–	–	65.27	–	7.02	7.12	1.66	24.55
R_{15}	0.7546	6.86	1.20	–	61.65	27.63	–	–	34.02	62.93	–	4.92	4.94	0.05	25.22

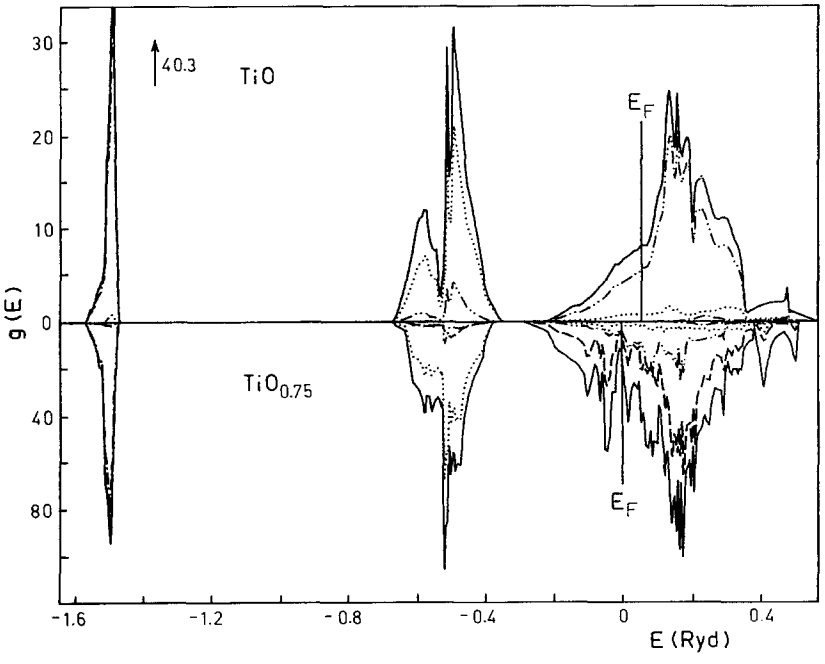

Fig. 3. Total DOS and main partial local DOS components for TiO and $TiO_{0.75}$ in units of states per Rydberg per spin and per unit cell. The curves are shifted to coincide at the bottom of the O 2s band. The Fermi level of $TiO_{0.75}$ is chosen as energy zero. ——: total DOS; –·–·–·–: O 2s DOS; ...: O 2p DOS; –··–: $Ti^{[6]}$ (Ti) 3d DOS; – – –: $Ti^{[4]}$ 3d DOS

and nitride, the introduction of vacancies causes a narrowing of the s and p bands, whereas the gap between these two bands remains almost unchanged. Quantitative details on band gaps and the relative positions of the Fermi levels for TiO and $TiO_{0.75}$ can be obtained from Table 3. While the introduction of vacancies into the carbide and nitride only causes a slight lowering of the Fermi energy (with respect to the bottom of the s band), the effect in the oxide is as large as 0.1 Ryd, thus indicating a relatively high stabilizing effect.

The partial local oxygen 2s and 2p and the $Ti^{[4]}$ and $Ti^{[6]}$ 3d DOS for $TiO_{0.75}$ as compared to the corresponding DOS for TiO are also displayed in Fig. 3. Two important features should be noticed. First, the areas of the oxygen 2s and 2p peaks are reduced by roughly a quarter, reflecting the smaller number of oxygen atoms per unit cell. This is accompanied by an almost proportional reduction of titanium 3d states in the oxygen 2p band, indicating a reduced number of bonds between oxygen 2p and titanium 3d states. Secondly, the vacancy peaks can be identified as $Ti^{[4]}$ 3d states. Both effects are similar in the carbide and in the nitride, except that the Fermi energy increases with respect to the vacancy peaks from the carbide to the oxide due to the increasing number of electrons.

Before proceeding further in the discussion of the DOS, the splitting of the p and d states in a crystal field of D_{4h} symmetry (which applies for oxygen and

Table 3. Band widths and band gaps (in Ryd.) for $TiO_{0.75}$ and for TiO

	Band	$TiO_{0.75}$	TiO
Band width	s	0.090	0.125
	p	0.295	0.326
	Occupied d (+vacancy)	0.285	0.299
Band gap	$s-p$	0.796	0.768
	$p-d$	0.087	0.130
E_F (with respect to bottom of s band)		1.554	1.648
E_F (with respect to bottom of p band)		0.638	0.755
E_F (with respect to muffin-tin zero)		0.831	0.949

$Ti^{[4]}$) shall be mentioned. For a qualitative picture see Fig. 2 of [16]. The $Ti^{[4]}$ $3d$ DOS is split into four different components, i.e. d_{z^2}, $d_{x^2-y^2}$, d_{xy} and (d_{xz}, d_{yz}), whereas states with p symmetry are split into the two components p_z and (p_x, p_y). For the description of the orbitals of the $Ti^{[4]}$ (oxygen) atom local coordinate systems have been introduced in which the z direction always points from the site of the $Ti^{[4]}$ (oxygen) atom to the adjacent vacancy ($Ti^{[6]}$ atom).

The local partial DOS in the vacancy sphere of $TiO_{0.75}$ is shown in the upper part of Fig. 4. In stoichiometric TiO three main bond types are found [23]: σ bonds between O $2p$ ($2s$) and Ti e_g states ($d_{x^2-y^2}$, d_{z^2}), π bonds between O $2p$ and Ti t_{2g} states (d_{xy}, d_{xz}, d_{yz}) and σ bonds between Ti t_{2g} states. In addition to these bond types, which also occur in $TiO_{0.75}$ and which will be discussed later, new bond types are caused by the oxygen vacancy. The $Ti^{[4]}$ d_{z^2} orbitals, and also the $Ti^{[4]}$ p_z orbitals, can form bonds across the oxygen vacancy designated as $Ti^{[4]}-\square_O-Ti^{[4]}$ bonds. An s character of the electrons in the vacancy sphere indicates the presence of *bonding* states with respect to the $Ti^{[4]}-\square_O-Ti^{[4]}$ bond, whereas p character indicates *antibonding* states. The wide peak at ca. -0.2 Ryd. is therefore dominated by bonding states which form $d_{z^2}-d_{z^2}$ σ bonds across the vacancy sphere. In the sharp peak below the Fermi level p character dominates which seems to originate from antibonding $Ti^{[4]}$ $3d$ states. The bonding states in this region seem to be caused by $Ti^{[4]}$ p_z states (see lower part of Fig. 4) which form p_z-p_z σ bonds across the vacancy sphere. A look at Table 2 shows that the vacancy state T_1 has a considerable amount of partial p charge besides a strikingly high (d_{xz}, d_{yz}) partial charge in the $Ti^{[4]}$ sphere but only a negligible charge in the $Ti^{[6]}$ sphere. Apart from the $Ti^{[4]}-\square_O-Ti^{[4]}$ p_z-p_z σ bond this state is involved in the $d-d$ σ

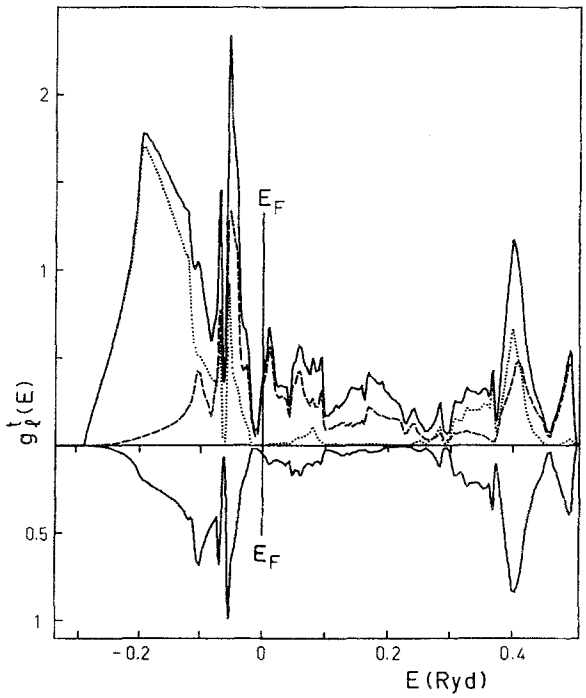

Fig. 4. Top: DOS in the vacancy sphere of ordered $TiO_{0.75}$. —: total DOS; ...: s-like DOS; – – –: p-like DOS. Bottom: p_z DOS in the $Ti^{[4]}$ sphere of ordered $TiO_{0.75}$. The same units as in Fig. 3 are used

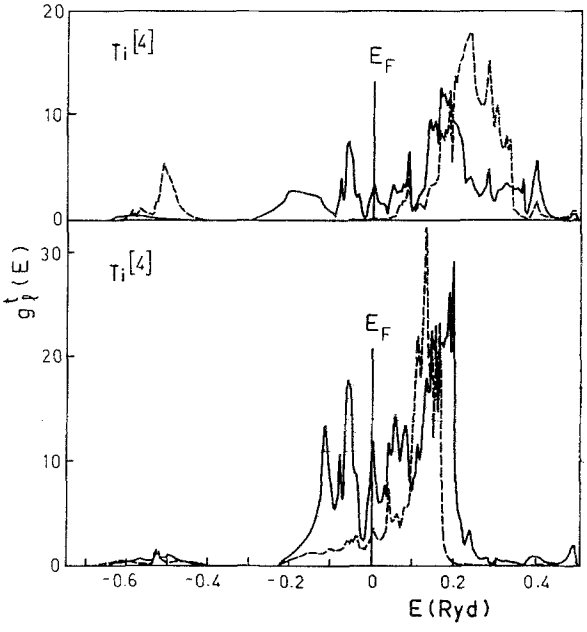

Fig. 5. Split of the partial $Ti^{[4]}$ $3d$ DOS in ordered $TiO_{0.75}$. Top: $Ti^{[4]}$ d_{z^2} (—) and $Ti^{[4]}$ $d_{x^2-y^2}$ (– – –) DOS. Bottom: $Ti^{[4]}$ (d_{xz}, d_{yz}) (—) and $Ti^{[4]}$ d_{xy} (– – –) DOS. The same units and energy zero as in Fig. 3 are used

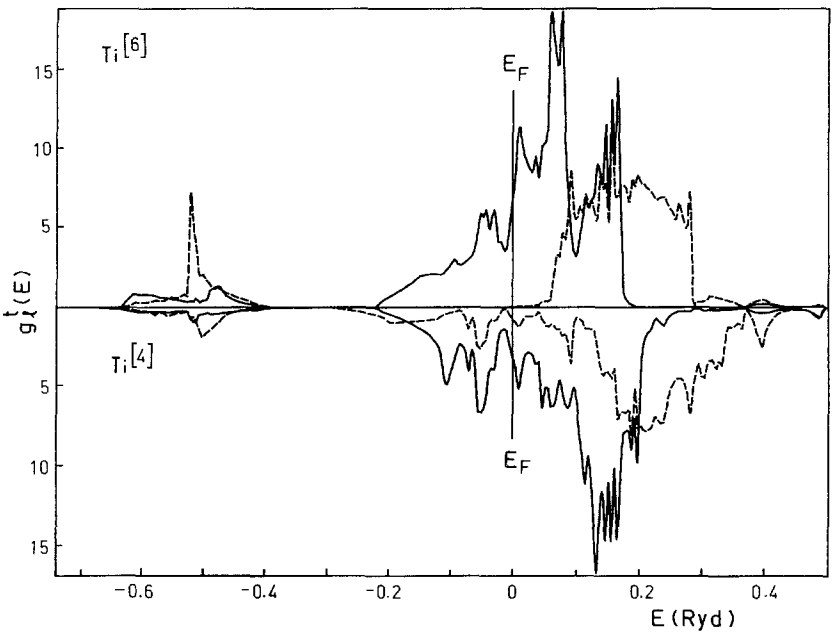

Fig. 6. Comparison of the $Ti^{[6]}$ t_{2g} (—) and e_g (– – –) DOS (top) with the respective sums of the $Ti^{[4]}$ (d_{xy}, d_{xz}, d_{yz}) (—) and the $Ti^{[4]}$ (d_{z^2}, $d_{x^2-y^2}$) (– – –) DOS (bottom). The partial $Ti^{[4]}$ DOS have been divided by three to refer to only one muffin-tin sphere. The same units and energy zero as in Fig. 3 are used

Table 4. LAPW partial charges and charge transfer between the superposition of atomic charges and the self-consistent LAPW calculation for ordered $TiO_{0.75}$ and for TiO (in electrons per atomic sphere)

		$TiO_{0.75}$					TiO		
Band		$Ti^{[4]}$	$Ti^{[6]}$	O	$\square_O$	interstitial	Ti	O	interstitial
s	*s*	0.01	0.02	1.69	–		0.02	1.66	
	p	0.02	0.03	–	–		0.08	–	
	d	0.02	0.04	–	–		0.03	–	
	total	0.06	0.10	1.70	–	0.16	0.14	1.66	0.20
p	*s*	0.07	0.09	0.01	0.01		0.09	0.01	
	p	0.11	0.16	3.86	0.01		0.17	3.89	
	d	0.35	0.66	0.01	–		0.57	0.01	
	total	0.56	0.95	3.88	0.02	0.93	0.87	3.91	1.22
d	*s*	0.04	–	–	0.42		–	–	
(+vacancy)	*p*	0.05	–	0.19	0.13		–	0.20	
	d	1.44	1.21	0.04	0.02		1.27	0.04	
	total	1.54	1.21	0.23	0.58	0.72	1.27	0.24	0.49
Occupied	*s*	0.12	0.11	1.71	0.43		0.11	1.66	
valence	*p*	0.18	0.19	4.04	0.14		0.24	4.09	
	d	1.83	1.91	0.04	0.02		1.87	0.05	
	total	2.17	2.27	5.80	0.60	1.81	2.28	5.81	1.19
Charge transfer		−0.19	−0.22	0.30	0.09	0.00	−0.18	0.29	−0.11

bonds between adjacent $Ti^{[4]}$ atoms and is probably responsible for the sharp peak in the vacancy DOS 0.07 Ryd. below the Fermi level.

The split of the $Ti^{[4]}$ 3*d* DOS into its four components is given in Fig. 5. In the upper part the components of the $Ti^{[4]}$ DOS which, in O_h, correspond to e_g states ("e_g"-like components) and in the lower part the components which correspond to t_{2g} states ("t_{2g}"-like components) are shown. While in TiO the Ti e_g states form σ bonds to the oxygen atoms, in $TiO_{0.75}$ the d_{z^2} component is involved in the $Ti^{[4]}$ $-Ti^{[4]}$ bonding across the vacancy and the $d_{x^2-y^2}$ component forms the $d-p$ σ (and $d-s$ σ) bonds to the remaining oxygen atoms. Therefore the d_{z^2} states are found mainly in the region of the vacancy peaks (i.e. in a region where no e_g states are found in TiO),

Table 5. Split of the partial Ti $3d$ charge in ordered $TiO_{0.75}$ and in TiO (in electrons per atomic sphere)

Band	$TiO_{0.75}$						TiO	
	$Ti^{[4]}$				$Ti^{[6]}$		Ti	
	d_{z^2}	$d_{x^2-y^2}$	d_{xy}	(d_{xz}, d_{yz})	e_g	t_{2g}	e_g	t_{2g}
p	0.03	0.19	0.07	0.08	0.44	0.26	0.38	0.23
d(+vacancy)	0.39	0.01	0.20	0.86	0.01	1.22	0.02	1.25
Occupied valence	0.43	0.21	0.27	0.94	0.49	1.47	0.44	1.48

in contrast to the $d_{x^2-y^2}$ states which contribute mainly to the oxygen $2p$ band.

Moreover, the titanium t_{2g} states in TiO, which form Ti–Ti d–d σ and Ti–O d–p π bonds, are changed in a characteristic fashion when the crystal field symmetry is lowered from O_h in TiO to D_{4h} in $TiO_{0.75}$. As regards the Ti–Ti bond, the (d_{xz}, d_{yz}) states form σ bonds between $Ti^{[4]}$ and $Ti^{[4]}$ atoms and the d_{xy} states σ bonds between $Ti^{[4]}$ and $Ti^{[6]}$ atoms. Although the "t_{2g}"-like DOS does not change considerably from Ti in TiO to $Ti^{[4]}$ in $TiO_{0.75}$, the main effect is the dominance of (d_{xz}, d_{yz}) states below the Fermi energy and a relatively high proportion of d_{xy} states above the Fermi energy indicating a reduced strength of the $Ti^{[4]}-Ti^{[6]}$ bonds compared with the $Ti^{[4]}-Ti^{[4]}$ bonds.

When one compares the e_g and t_{2g} DOS of $Ti^{[6]}$ with the sum of the "e_g"- and "t_{2g}"-like components of $Ti^{[4]}$ (Fig. 6) the significant difference is the presence of "e_g"-like $Ti^{[4]}$ states in the d band below the Fermi energy caused by the vacancy states and the $Ti^{[4]}-\square_O-Ti^{[4]}$ bonds. The reduction of "e_g"-like $Ti^{[4]}$ DOS in the p band compared to the e_g component of the $Ti^{[6]}$ DOS is due to the reduced number of Ti–O bonds formed by $Ti^{[4]}$.

b) Partial charges and charge transfer

Table 4 displays the charge transfer, defined as the difference between the self-consistent LAPW charges and the superposed (neutral) atomic charges, for the muffin-tin spheres and in the interstitial region of TiO and $TiO_{0.75}$.

In both TiO and $TiO_{0.75}$ there is a charge transfer from the titanium to the oxygen sphere. In the series TiC–TiN–TiO and $TiC_{0.75}-TiN_{0.75}-TiO_{0.75}$ a trend to less pronounced charge transfers is observed. The gain of charge in the vacancy sphere during the self-consistency cycle is slightly more pronounced in the oxide than in the nitride, whereas a loss of charge occurs for the carbide. These small effects illustrate the growing strength of the $Ti^{[4]}-Ti^{[4]}$ bonds across the vacancy, an effect more distinct between $TiC_{0.75}$ and $TiN_{0.75}$ than between $TiN_{0.75}$ and $TiO_{0.75}$.

Table 4 also presents the local partial s, p and d charges for the occupied valence bands of $TiO_{0.75}$ and TiO. The charges are given in electrons per muffin-tin sphere and, in order to facilitate the comparison with TiO, refer to only a quarter of the interstitial volume of the simple cubic unit cell for $TiO_{0.75}$. The most drastic changes in $TiO_{0.75}$ as compared to TiO, i.e. the decrease of $Ti^{[4]}$ charge and interstitial charge in the p band and an increase of those charges in the d band, are similar to the corresponding effects in the carbide and nitride and reflect the reduced number of titanium-non-metal bonds and the higher number of titanium-titanium bonds. The absolute figures also reveal the weakening of titanium-non-metal bonds and the strengthening of titanium-titanium bonds in the series from the carbide to the oxide.

Table 6. Partial charges (in percent) for the states involved in the $Ti^{[4]}-Ti^{[6]}$ bonding in $TiC_{0.75}$ [16], $TiN_{0.75}$ [17] and $TiO_{0.75}$

Irr. rep.		E(Ryd.)	$Ti^{[4]}d_{xy}$	$Ti^{[6]}t_{2g}$	q_{out}
$\Gamma_{25'}$	$TiC_{0.75}$	0.547	16.20	17.38	39.75
	$TiN_{0.75}$	0.630	10.04	20.20	36.00
	$TiO_{0.75}$	0.615	15.17	21.35	36.33
$\Gamma_{25'}$	$TiC_{0.75}$	0.714	16.50	17.77	19.79
	$TiN_{0.75}$	0.823	10.13	19.99	22.83
	$TiO_{0.75}$	0.816	10.93	21.58	20.71
$X_{2'}$	$TiC_{0.75}$	0.612	31.49	33.80	30.64
	$TiN_{0.75}$	0.695	24.12	39.96	33.85
	$TiO_{0.75}$	0.687	26.39	39.42	31.06

A split of the Ti $3d$ charges into the contributions from the p and the d (+vacancy) bands (Table 5) provides further information on the bonding situation. Although the charge components in the $Ti^{[6]}$ sphere are very similar to those of Ti in TiO, the main effects occur for the $Ti^{[4]}$ $3d$ states in the d band where the vacancy states of d_{z^2} ("e_g"-like) symmetry appear which form $Ti^{[4]}-Ti^{[4]}$ bonds across the vacancy. The decrease of "t_{2g}"-like charge for $Ti^{[4]}$ in the d band is mainly due to the d_{xy} states and is related to the weakening of the $Ti^{[4]}-Ti^{[6]}$ bond compared with the Ti–Ti bond in TiO.

In this context it is interesting to compare the $Ti^{[4]}-Ti^{[6]}$ bonds in the series $TiC_{0.75}-TiN_{0.75}-TiO_{0.75}$. If the local partial charges for a mesh of only four **k** points (Γ, X, M, R) are taken, there are only three different states which have $Ti^{[4]}$ d_{xy} and $Ti^{[6]}$ t_{2g} character. Those states are listed in Table 6. In the carbide only the two lowest states are below the Fermi energy, in the nitride the state $\Gamma_{25'}$ at 0.823 Ryd. is almost exactly

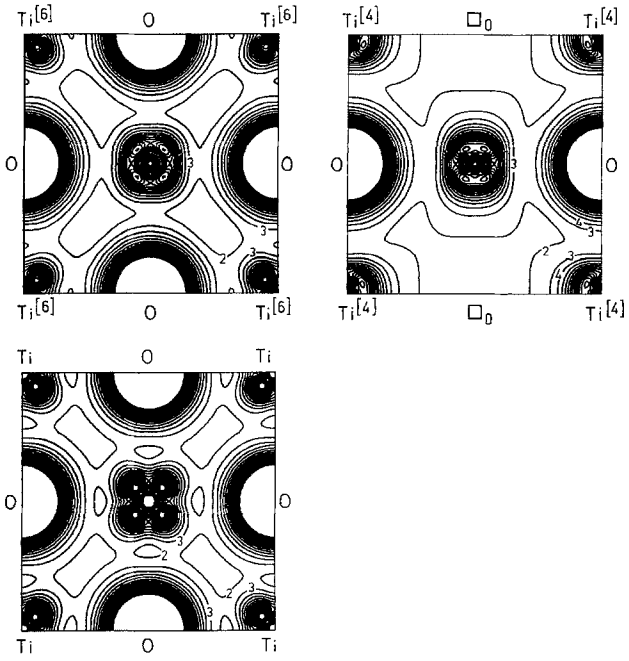

Fig. 7. Valence electron densities in the (100) plane of $Ti_3^{[4]}Ti^{[6]}O_3\square_O$ and TiO in units of $10^{-1}e/Å^3$. Left: $TiO_{0.75}$, cut 1; centre: $TiO_{0.75}$, cut 2; right: TiO

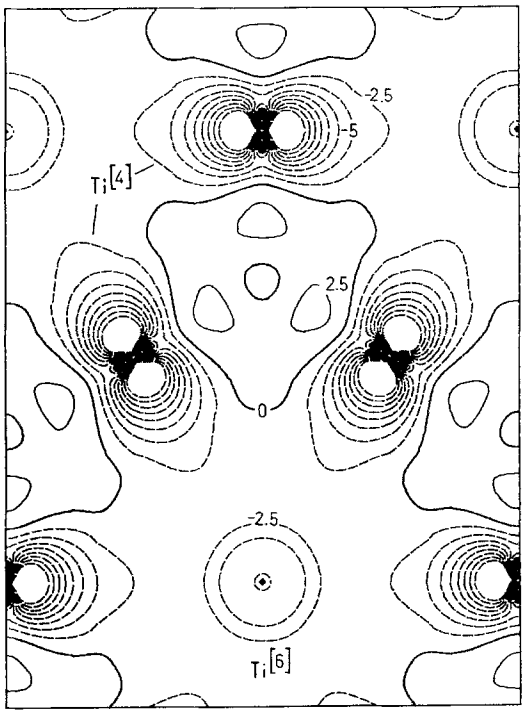

Fig. 9. Difference between the valence electron densities of $TiO_{0.75}$ and TiO (omitting the 2*s* band) for the (111) plane in units of $10^{-2}e/Å^3$

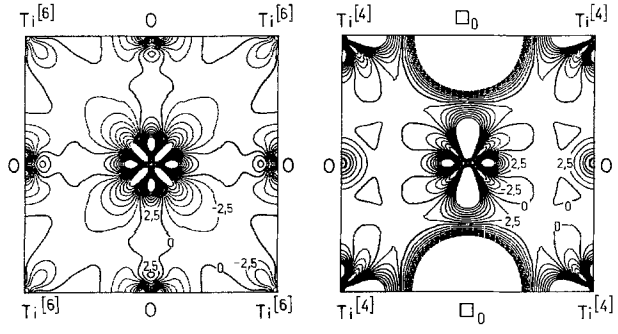

Fig. 8. Difference between the valence electron densities of $TiO_{0.75}$ and TiO (omitting the 2*s* band) for the two different cuts in the (100) plane in units of $10^{-2}e/Å^3$

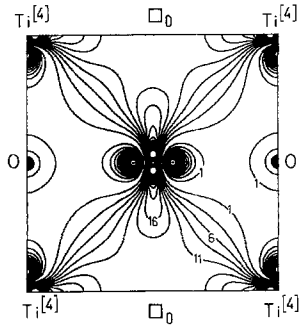

Fig. 10. Electron density for the "vacancy band" state Γ_1 of $TiO_{0.75}$ in the (100) plane (cut 2) in units of $10^{-2}e/Å^3$

at the Fermi level whereas in the oxide all three states are below E_F. This means, in absolute terms, that the strength of the $Ti^{[4]}-Ti^{[6]}$ bond increases from $TiC_{0.75}$ to $TiO_{0.75}$.

c) Electron densities

The valence electron densities of $TiO_{0.75}$ for the two inequivalent cuts in the (100) plane together with the corresponding plot for TiO are presented in Fig. 7. The two important features exhibited by these density plots are the strengthening of the $Ti^{[4]}-O$ bond and the weakening of the $Ti^{[4]}-Ti^{[6]}$ bond in $TiO_{0.75}$ as compared to TiO. A more detailed analysis of the changing bond strength caused by the introduction of non-metal vacancies can be obtained from density difference plots in the (100) plane (Fig. 8) and in the (111) plane (Fig. 9), where the valence electron density (without the contribution from the *s* band) of TiO is subtracted from the corresponding density of $TiO_{0.75}$. Apart from the already mentioned strengthening of the $Ti^{[4]}-O$ bond and the weakening of the $Ti^{[4]}-Ti^{[6]}$ bond the following other changes are noticed: (*i*) a weakening of the $Ti^{[4]}-Ti^{[4]}$ bonds, (*ii*) $Ti^{[4]}-\square_O-Ti^{[4]}$ bonds which are apparently stronger than the Ti–O–Ti bonds in TiO and (*iii*) a reduced electron density at the oxygen atom in direction of the $Ti^{[6]}$ atom, thus leading to a weaker $Ti^{[6]}-O$ bond than in TiO.

While in the stoichiometric compound the principal covalent bond types are the Ti–O $d-p$ σ and $d-p$ π as well as the Ti–Ti $d-d$ σ bonds [23], $Ti^{[4]}-\square_O$

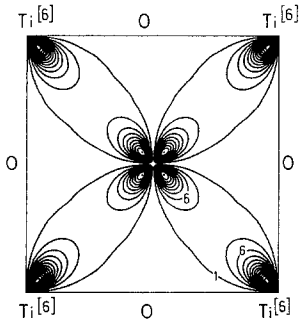

Fig. 11. Electron density of the state $\Gamma_{25'}$ of $TiO_{0.75}$ in the (100) plane (cut 1) in units of $10^{-2} e/Å^3$

$-Ti^{[4]}$ $d-d$ σ bonds are formed by the introduction of oxygen vacancies. They are illustrated in Fig. 10 by the electron density of the vacancy state Γ_1. To a lesser extent also $p-p$ σ bonds across the vacancy are formed mainly by state R_1 (see Table 2).

The introduction of vacancies also influences the bonds between the six $Ti^{[4]}$ atoms octahedrally surrounding the vacancy. These bonds are formed by (d_{xz}, d_{yz}) states. An example for a bonding state of that type is the state X_3 whose electron density is very similar to the corresponding electron density in $TiN_{0.75}$ which can be found in Fig. 13 of [17]. In contrast to the carbide and the nitride, however, these bonds are weaker in $TiO_{0.75}$ as compared to TiO, although the absolute bond strength increases both from TiC to TiO and from $TiC_{0.75}$ to $TiO_{0.75}$.

A similar but more pronounced trend is found for the $Ti^{[4]}-Ti^{[6]}$ bond which is illustrated in Fig. 11 by the electron density for the state $\Gamma_{25'}$ (at 0.615 Ryd.; see Table 6). Also for this bond the absolute strength increases from the carbide to the oxide, but, when considered relative to the stoichiometric compounds, it is stronger only for the carbide but becomes increasingly weaker for the nitride and for the oxide.

4. Conclusion

Although the present calculation is based only on a model structure which is not observed experimentally, it nevertheless provides valuable, though more qualitative, insight into the vacancy induced changes in the bonding situation of titanium oxide and, together with the results of previous calculations on $TiC_{0.75}$ [15, 16] and $TiN_{0.75}$ [17], also for the series from titanium carbide to titanium oxide.

By comparing the stoichiometric compounds TiC, TiN and TiO, one notices pronounced changes in the bonding mechanism. While in TiC the titanium-carbon bonding is of predominant importance, the situation changes when going to the nitride and the oxide, where the titanium-titanium bonding becomes dominating. The introduction of non-metal vacancies has a different influence on the relative bond strengths for the three compounds. Generally speaking, the $Ti^{[4]}-Ti^{[6]}$ bonds are weaker than the $Ti^{[4]}-Ti^{[4]}$ bonds in the substoichiometric compounds because in the crystal field of D_{4h} symmetry the d_{xy} states are shifted to higher energies (see Fig. 2 of Ref. 16) and are therefore not all occupied.

The loss of stabilization energy in the carbide by the breaking up of the Ti–C bonds is compensated by stronger $Ti^{[4]}-Ti^{[4]}$ and $Ti^{[4]}-Ti^{[6]}$ bonds. A removal of titanium atoms would have a destabilizing effect. The same is still true for the nitride where the $Ti^{[4]}-Ti^{[6]}$ bonds are weakened but where the covalent $Ti^{[6]}-N$ bonding is still strong enough, so that no Ti vacancies are found experimentally.

In the oxide, on the other hand, both the $Ti^{[4]}-Ti^{[4]}$ bonds and the $Ti^{[4]}-Ti^{[6]}$ bonds are weakened by the introduction of vacancies. While the $Ti^{[4]}$ atoms, despite their loss of two oxygen neighbours, are stabilized by forming stronger $Ti^{[4]}-\square_O-Ti^{[4]}$ as well as $Ti^{[4]}-O$ bonds, the $Ti^{[6]}$ atoms neither form sufficiently strong bonds to the $Ti^{[4]}$ nor to the oxygen atoms, so that a structure with vacancies on both sublattices is more stable.

We gratefully acknowledge financial support by the "Hochschuljubiläumsstiftung der Stadt Wien".

References

1. Murray, J.L., Wriedt, H.A.: Bull. Alloy Phase Diagr. **8**, 148 (1987)
2. Watanabe, D., Castles, J.R., Jostsons, A., Malin, A.S.: Acta Crystallogr. **23**, 307 (1967)
3. Hilti, E.: Naturwissenschaften **55**, 130 (1968)
4. Banus, M.D., Reed, T.B., Strauss, A.J.: Phys. Rev. B**5**, 2775 (1972)
5. Bilz, H.: Z. Physik **153**, 338 (1958)
6. Yamashita, J.: J. Phys. Soc. Jpn. **18**, 1010 (1963)
7. Honig, J.M., Wahnsiedler, W.E., Dimmock, J.O.: J.: Solid State Chem. **5**, 452 (1972)
8. Ern, V., Switendick, A.C.: Phys. Rev. **137**, 202 (1965)
9. Mattheiss, L.F.: Phys. Rev. B**5**, 290 (1972)
10. Neckel, A., Rastl, P., Eibler, R., Weinberger, P., Schwarz, K.: J. Phys. C: Solid State Phys. **9**, 579 (1976)
11. Schoen, J.M., Denker, S.P.: Phys. Rev. **184**, 864 (1969)
12. Burdett, J.K., Hughbanks, T.: J. Am. Chem. Soc. **106**, 3101 (1984)
13. Schwarz, K.: Phys. Chem. Minerals **14**, 315 (1987)
14. Hörmandinger, G., Redinger, J., Weinberger, P., Hobiger, G., Herzig, P.: Solid State Commun. **68**, 467 (1988)
15. Redinger, J., Eibler, R., Herzig, P., Neckel, A., Podloucky, R., Wimmer, E.: J. Phys. Chem. Solids **46**, 383 (1985)
16. Redinger, J., Eibler, R., Herzig, P., Neckel, A., Podloucky, R., Wimmer, E.: J. Phys. Chem. Solids **47**, 387 (1986)
17. Herzig, P., Redinger, J., Eibler, R., Neckel, A.: J. Solid State Chem. **70**, 281 (1987)
18. Hobiger, G., Herzig, P., Eibler, R., Schlapansky, F., Neckel, A.: J. Phys.: Condensed Matter (submitted for publication)
19. Andersen, O.K.: Phys. Rev. B**12**, 3060 (1975)
20. Koelling, D.D., Arbman, G.O.: J. Phys. F: Met. Phys. **5**, 2041 (1975)
21. Hedin, L., Lundqvist, S.: J. Phys. Paris **33**, C3–73 (1972)
22. Lehmann, G., Taut, M.: Phys. Status Solidi (b) **54**, 469 (1972)
23. Neckel, A., Schwarz, K., Eibler, R., Weinberger, P., Rastl, P.: Ber. Bunsenges. Phys. Chem. **79**, 1053 (1975)

F. Schlapansky, P. Herzig, R. Eibler, G. Hobiger, A. Neckel
Institut für Physikalische Chemie
Universität Wien
Währingerstrasse 42
A-1090 Vienna
Austria